

Electronic Supplementary Information

Direct observation of crystal degradation behaviour in porous crystals under low-dose electron diffraction conditions

Hikaru Sakamoto and Masataka Ohtani^{†,*}

[†] School of Environmental Science and Engineering, Kochi University of Technology

185 Miyanokuchi, Tosayamada, Kami, Kochi 782-8502, Japan

E-mail: ohtani.masataka@kochi-tech.ac.jp (M.O.)

Table of Contents

1. Materials	S2
2. Experimental Procedure	S2
3. Data Analysis	S5
4. Supporting Figures	S6

1. Materials

All the reagents and chemicals used were obtained from commercial sources and used as received, unless otherwise noted. Methanol (MeOH), *N,N*-dimethylformamide (DMF), acetonitrile (MeCN), zinc (II) nitrate hexahydrate ($\text{Zn}(\text{NO}_3)_2 \cdot 6\text{H}_2\text{O}$), 1-methylimidazole (1-MIm), 2-methylimidazole (2-HMIm), benzimidazole (HBIm), cobalt (II) nitrate hexahydrate ($\text{Co}(\text{NO}_3)_2 \cdot 6\text{H}_2\text{O}$), zirconium (IV) chloride (ZrCl_2), zirconium (IV) tetrapropoxide (ca. 70% in *n*-propanol_ $\text{Zr}(\text{O}^i\text{Pr})_4$), titanium (IV) tetraisopropoxide ($\text{Ti}(\text{O}^i\text{Pr})_4$), terephthalic acid (BDC), 2-aminoterephthalic acid (BDC-NH₂), 2,5-dibromoterephthalic acid (BDC-Br₂), 4,4'-biphenyldicarboxylic acid, acetic acid, L-histidine were purchased from Wako Pure Chemical Industries Co. Ltd (Japan).

2. Experimental Procedure

2.1 Synthesis of ZIF-8 nanocrystals.

734.4 mg (2.47 mmol) of $\text{Zn}(\text{NO}_3)_2 \cdot 6\text{H}_2\text{O}$ and 810.6 mg (9.87 mmol) of 1-MIm were dissolved in MeOH (50 mL). A second solution is prepared by dissolving 810.6 mg (9.87 mmol) of 2-HMIm and 249 mg (2.47 mmol) of TEA in MeOH (50 mL). The latter clear solution is poured into the former clear solution under stirring min with a magnetic stirrer (25 °C, 5 min). After 24 h, the obtained mixture was centrifuged (9,000 rpm, 15 min), washed several times with MeOH and MeCN, and dried under vacuum (30 °C, 24 hour) to give a powdery product (white powder).

2.2 Synthesis of ZIF-7 nanocrystals.

300 mg (1.01 mmol) of $\text{Zn}(\text{NO}_3)_2 \cdot 6\text{H}_2\text{O}$ were dissolved in DMF (50 mL). A second solution is prepared by dissolving 770 mg (6.51 mmol) of HBIm in DMF (50 mL). The latter clear solution is poured into the former clear solution under stirring 5 min with a magnetic stirrer (25 °C). After 2 days, the obtained mixture was centrifuged (9,000 rpm, 15 min), washed several times with DMF, and dried under vacuum (30 °C, 24 hour) to give a powdery product (white powder).

2.3 Synthesis of ZIF-67 nanocrystals.

718.8 mg (2.47 mmol) of $\text{Co}(\text{NO}_3)_2 \cdot 6\text{H}_2\text{O}$ and 810.6 mg (9.87 mmol) of 1-MIm were dissolved in MeOH (50 mL). A second solution is prepared by dissolving 810.6 mg (9.87 mmol) of 2-HMIm and 96.6 (0.69 mmol) of TEA in MeOH (50 mL). The latter clear solution is poured into the former

clear solution under stirring 5 min with a magnetic stirrer (25 °C). After 20 h, the obtained mixture was centrifuged (9,000 rpm, 15 min), washed several times with MeOH and MeCN, and dried under vacuum (30 °C, 24 hour) to give a powdery product (purple powder).

2.4 Synthesis of UiO-66 and Ti(30%) doped UiO-66 nanocrystals.

Zr(OⁿPr)₄ (2 mmol) and acetic acid (0.4 mmol) were dissolved in DMF (30 mL). The zirconium solution is stirred for 2 hours at room temperature. A second solution is prepared by dissolving BDC (4 mmol) in DMF (30 mL). The latter clear solution is poured into the former clear solution under stirring for 1 hour with a magnetic stirrer (25 °C). After 20 h, the obtained mixture was centrifuged (9,000 rpm, 15 min), washed several times with DMF and MeOH, and dried under vacuum (30 °C, 24 hour) to give a powdery product (white powder).

The procedure for the synthesis of Ti(30%)-doped UiO-66 is the same as that described above, except for dissolving Ti(OⁿPr)₄ in the first solution and reaction temperature (130 °C).

2.5 Synthesis of UiO-66-NH₂ and UiO-66-Br₂ nanocrystals.

ZrCl₄ (1.3 mmol) and acetic acid (87.4 mmol), deionized water (1 mmol) were dissolved in DMF (15 mL). A second solution is prepared by dissolving BDC-NH₂ (or BDC-Br₂_1.3 mmol) in DMF (15 mL). The latter clear solution is poured into the former clear solution and heated at 130 °C for 20 hours. The obtained mixture was centrifuged (9,000 rpm, 15 min), washed several times with DMF and MeOH, and dried under vacuum (30 °C, 24 hour) to give a powdery product (white powder).

2.6 Synthesis of UiO-67 nanocrystals.

ZrCl₄ (0.65 mmol) and acetic acid (43.7 mmol), deionized water (0.65 mmol) were dissolved in DMF (7.5 mL). A second solution is prepared by dissolving 4,4'-biphenyldicarboxylic acid in DMF (7.5 mL). The latter clear solution is poured into the former clear solution under stirring at 120 °C. After 24 hours, the obtained mixture was centrifuged (9,000 rpm, 15 min), washed several times with DMF and MeOH, and dried under vacuum (30 °C, 24 hour) to give a powdery product (faint yellow powder).

2.7 Scanning Electron Microscopy

Scanning electron microscopy (SEM) images were measured on a Hitachi FE-SEM SU-8020 scanning electron microscope. A SEM sample was prepared by dropping dispersion liquid on a non-refractive silicon wafer.

2.8 Powder X-ray diffraction (XRD) measurement

Powder X-ray diffraction (XRD) measurements were performed using a Rigaku SmartLab SE diffractometer with graphite-monochromatized Cu- K_{α} radiation (X-ray wavelength: 1.5418 Å) in steps of 0.01° over the 2θ range of 5–60°. A sample was set in a non-refractive silicon holder.

2.9 Thermogravimetric (TG) measurement

The thermogravimetric (TG) analysis was measured on a HITACHI STA7200RV. A sample was placed on an open platinum sample pan. The experiments were conducted at 1 °C/min heating in air.

2.10 Electron diffraction and TEM image collection

Transmission electron microscope (TEM) images were collected using a JEM-ARM200F “NEO ARM” (Gatan Rio 16 detector). For the preparation of the specimen, first, the powdery sample was dispersed in MeOH with sonication (30 min). Then, 5 μ L of resultant dispersion was drop-casted on a carbon coated copper microgrid and the solvent was vaporized under vacuum. The post-dried TEM grids were then fixed in a sample holder for observation, and the sample-equipped holder was evacuated overnight (> 12 h) under vacuum conditions (< 1×10^{-5} Pa).

Electron diffraction experiments were performed under a parallel electron illumination with acceleration voltage of 200 kV. We used an electron beam of 50 μ m (CL aperture) in diameter with an estimated total electron dose rate of 0.01-0.05 $e^{-}/\text{Å}^2 \cdot \text{s}$. We used a selective area aperture of 100 μ m in diameter to choose the region from which diffraction patterns were collected. TEM/Shadow imaging mode was used for particle searching. As soon as suitable particles are located, the electron beam is blanked to avoid unnecessary electron dose. Electron diffraction patterns were collected continuously using pixel detector (TVIPS XF416R, 2048 x 2048 pixels). The pixel size of the electron diffraction pattern has been carefully calibrated for each camera length that was used in the experiment. To correct for camera length, CeO₂ was used as a standard material.

a (pA/cm²): Value of current density on a fluorescent plate, M : magnification, t (sec) : exposure time

$$(\text{total electron dose}) = \frac{a \cdot M^2 \cdot t}{1.602} \times 10^{-9} \left[\frac{e^{-}}{\text{Å}^2} \right]$$

3. Data Analysis

- **Quantitatively evaluation of electron beam damage to materials**

Diffraction measurements of each samples took at around 300 K with acceleration voltage of 200 kV. In total, 10-15 diffraction patterns were taken at the same spot (size of the selected area aperture: 100 μm in diameter) using an exposure time of 10 s/pattern. The evaluation of brightness of each diffraction spot were performed by using Image J. The average brightness (brightness/pixel) was calculated by dividing the brightness of the selected area centered the diffraction spots by the number of pixels. Furthermore, the average brightness of each diffracted spot was normalized based on the average brightness of each diffraction spot with a beam irradiation time of 0 minute.

The diffraction rings intensity related to the time course of beam-induced decomposition was angular integrated by using Fit2d software. The camera length was corrected for each sample by using commercially available cerium oxide as a standard sample. The diffraction data converted from two-dimensional to one-dimensional by Fit2d was output on a graph with the horizontal axis 2θ and the vertical axis integrated intensity. The peak area was calculated by adapting a polynomial regression curve to the diffraction pattern for each time period using Igor, a data analysis software. The total peak area is the sum of the areas of all diffraction peaks, except for the diffraction peak that appears at the lowest angle (number 0). The diffraction peaks at high angle weren't detected by the automatic peak detection due to their weak intensity. Therefore, the peak areas were calculated within the fitting range. In order to investigate the time course of peak area, the vertical axis was standardized based on the total peak area immediately after electron irradiation.

4. Supporting Figures

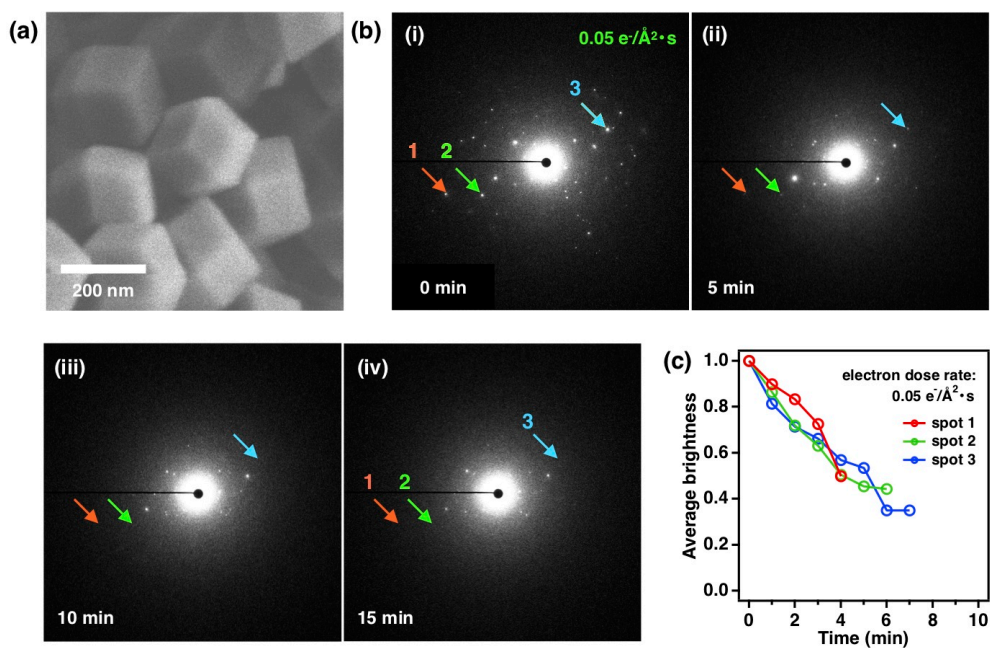


Figure S1. (a) A SEM image of 200 nm-sized ZIF-8 crystal, (b) electron diffraction images, and (c) the time course change of diffraction spot intensities (electron dose rate: 0.05 e⁻/Å²·s).

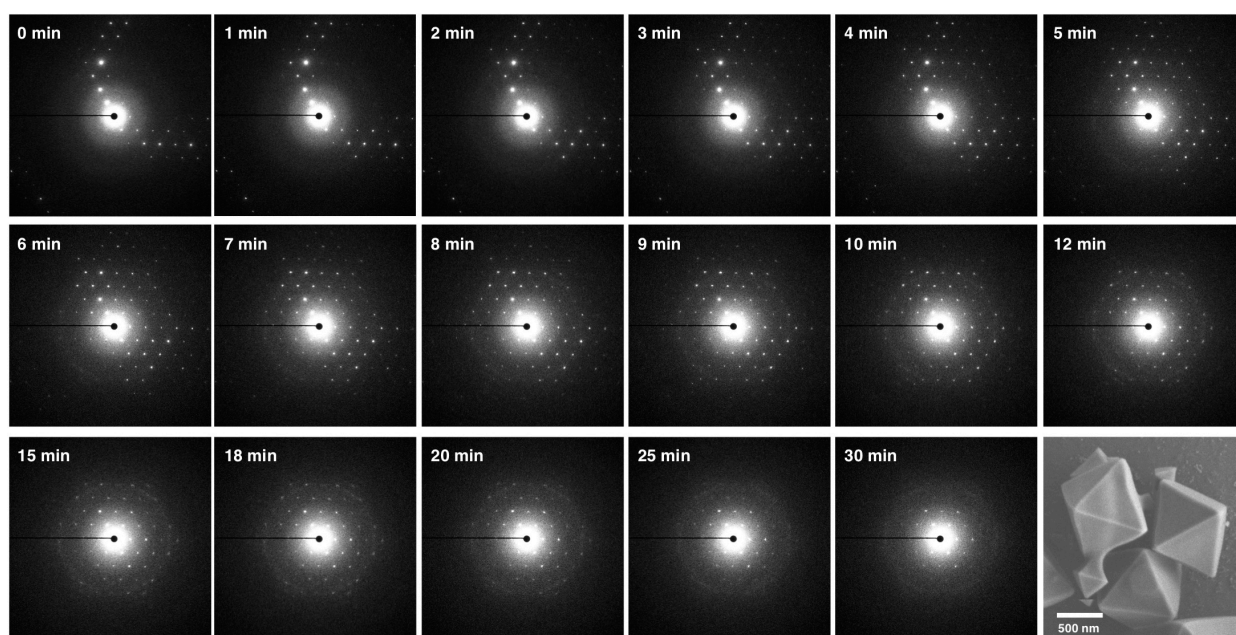


Figure S2. Electron diffraction image of a single UiO-66 crystal with different irradiation time and SEM image.

Table S1. Combination of metal ions and ligands in each MOF.

entry	metal ion	ligand
MAF-6	Zn ²⁺	2-ethylimidazolate
ZIF-8	Zn ²⁺	2-methylimidazolate
ZIF-67	Co ²⁺	2-methylimidazolate
ZIF-7	Zn ²⁺	benzimidazole
UiO-66	Zr ⁴⁺	terephthalate
Ti doped UiO-66	Ti ⁴⁺ /Zr ⁴⁺	terephthalate
UiO-66-NH ₂	Zr ⁴⁺	2-aminoterephthalate
UiO-66-Br ₂	Zr ⁴⁺	2,5-dibromoterephthalate
UiO-67	Zr ⁴⁺	4,4'-biphenyldicarboxylic acid

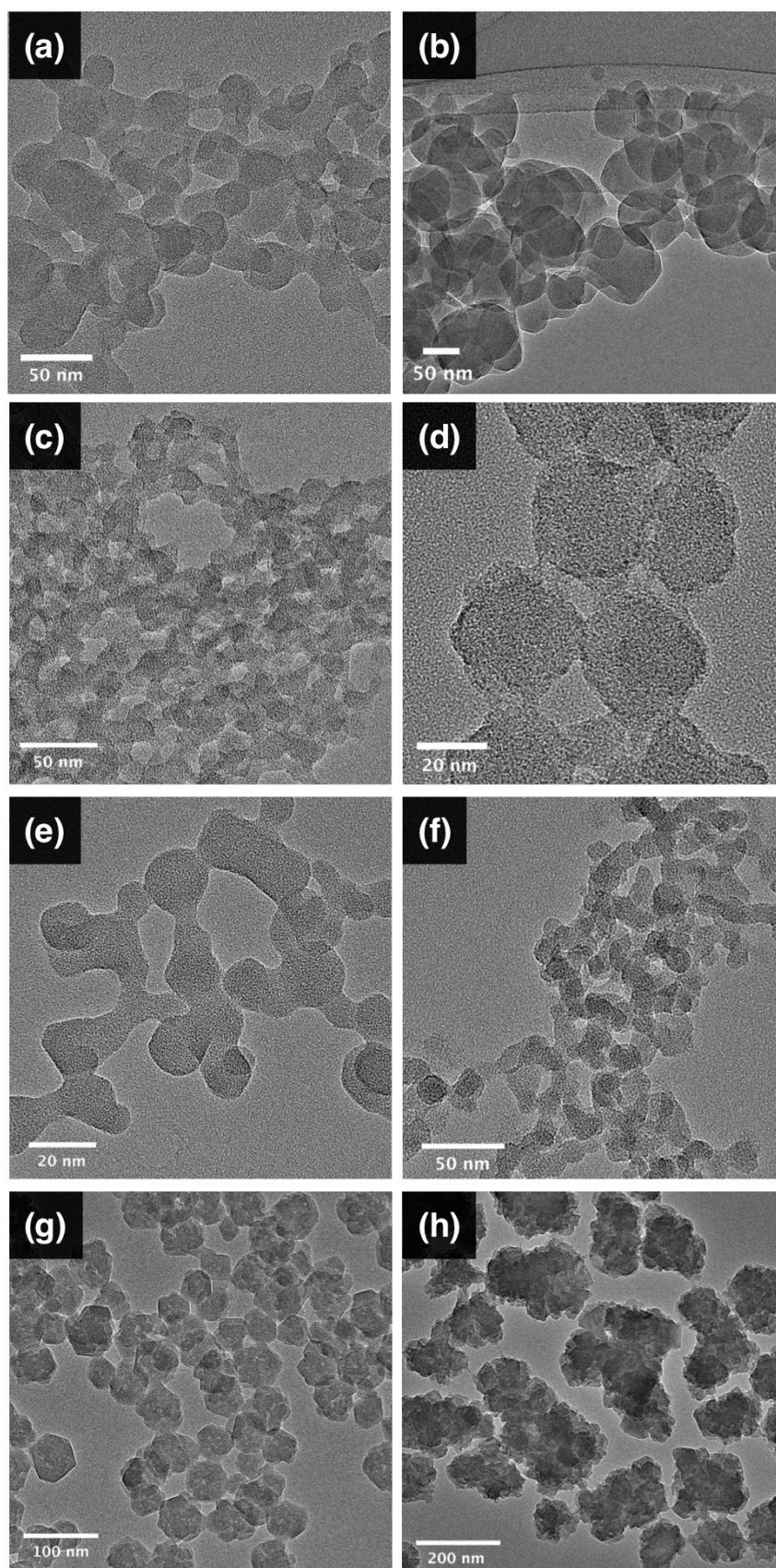


Figure S3. TEM images of the samples with controlled crystal size below 50 nm: (a) ZIF-67, (b) MAF-6, (c) UiO-66, (d) Ti-doped UiO-66, (e) UiO-66_NH₂, (f) UiO-66-Br₂, (g) ZIF-7, and (h) UiO-67.

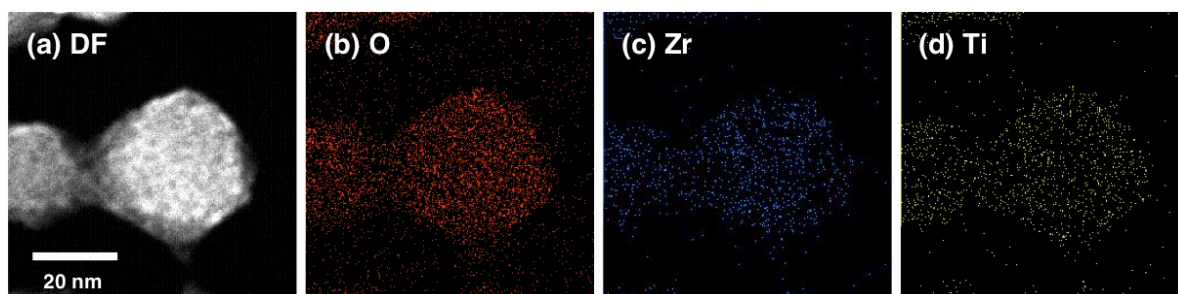


Figure S4. (a) STEM DF image and (b–d) EDX element mapping images of Ti-doped UiO-66 (Table S2).

Table S2. Summary of STEM-EDX analysis of Ti doped UiO-66.

Entry #1			
element	count	wt %	at %
Ti K	2765	18.7	30.5
Zr K	2193	81.3	69.5
sum		100	100
Entry #2			
element	count	wt %	at %
Ti K	3060	20.0	32.3
Zr K	2230	80.0	67.7
sum		100	100
Entry #3			
element	count	wt %	at %
Ti K	1124	18.3	29.9
Zr K	917	81.7	70.1
sum		100	100

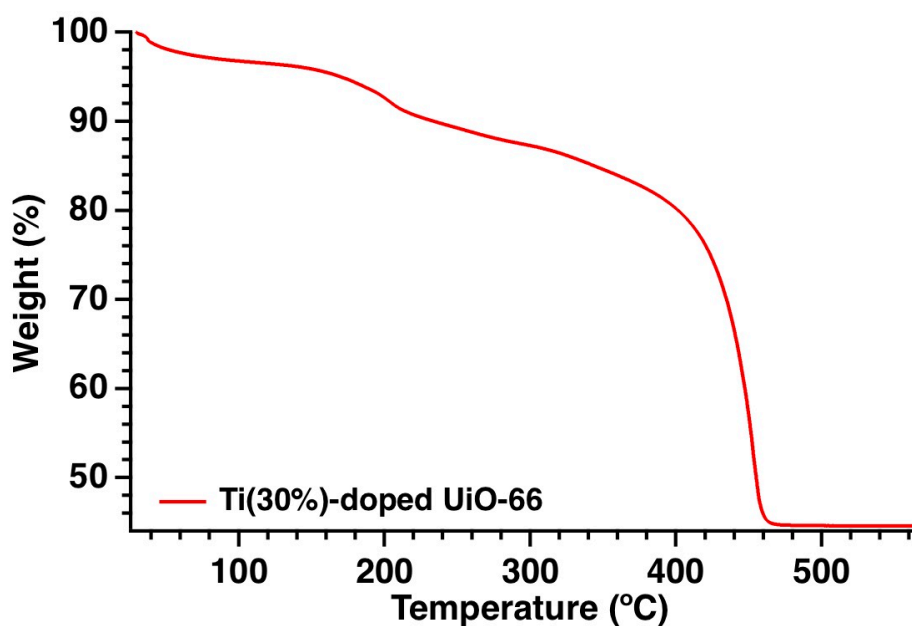


Figure S5. TGA curve of Ti(30%)-doped UiO-66. In a case, the heating ramp was of 1 °C/min in air flow (100 mL/min).

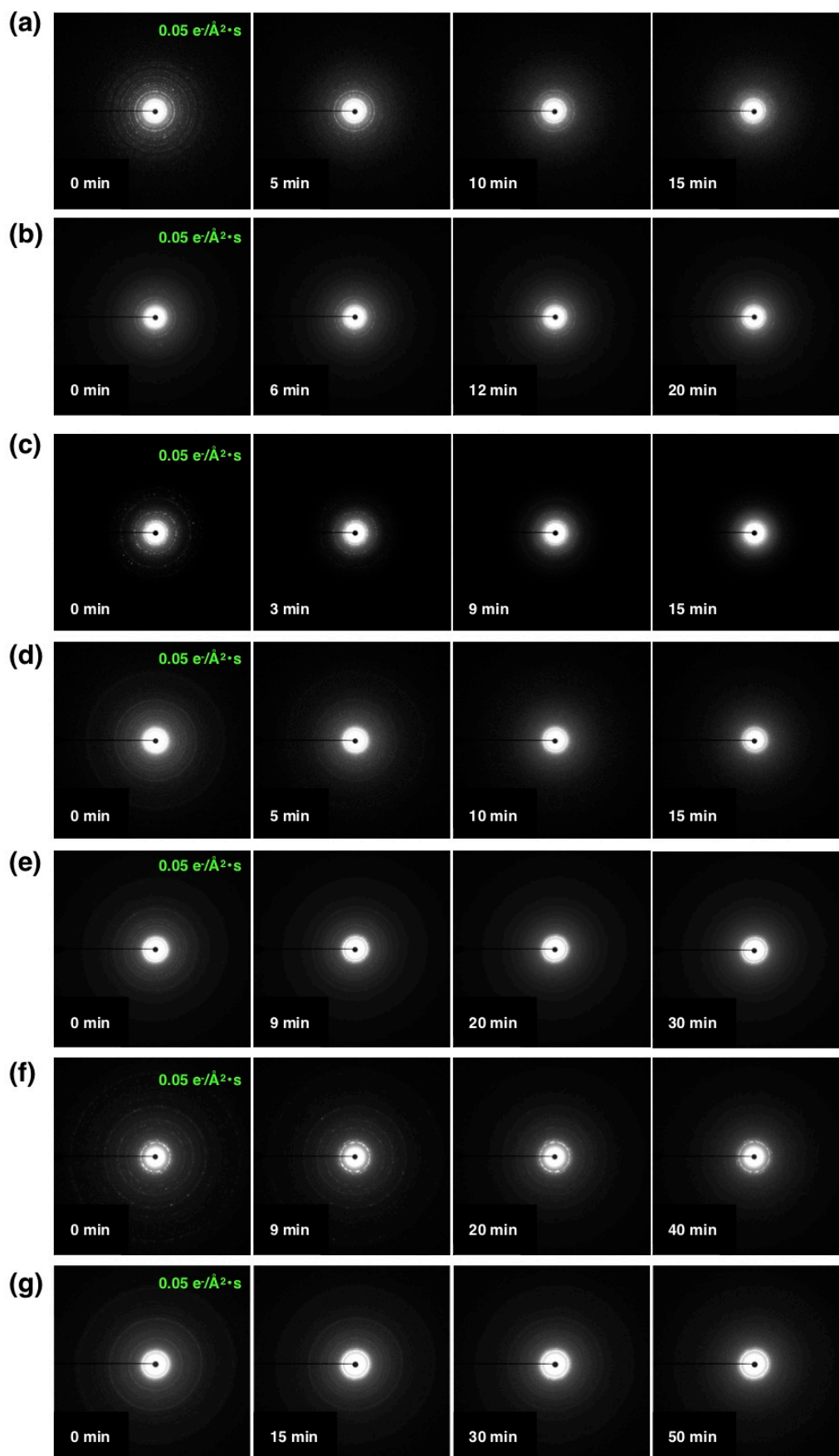


Figure S6. Electron diffraction image of samples with different irradiation time: (a) ZIF-8, (b) ZIF-67, (c) MAF-6, (d) UiO-66, (e) Ti-doped UiO-66, (f) UiO-66-NH₂, and (g) UiO-66-Br₂.

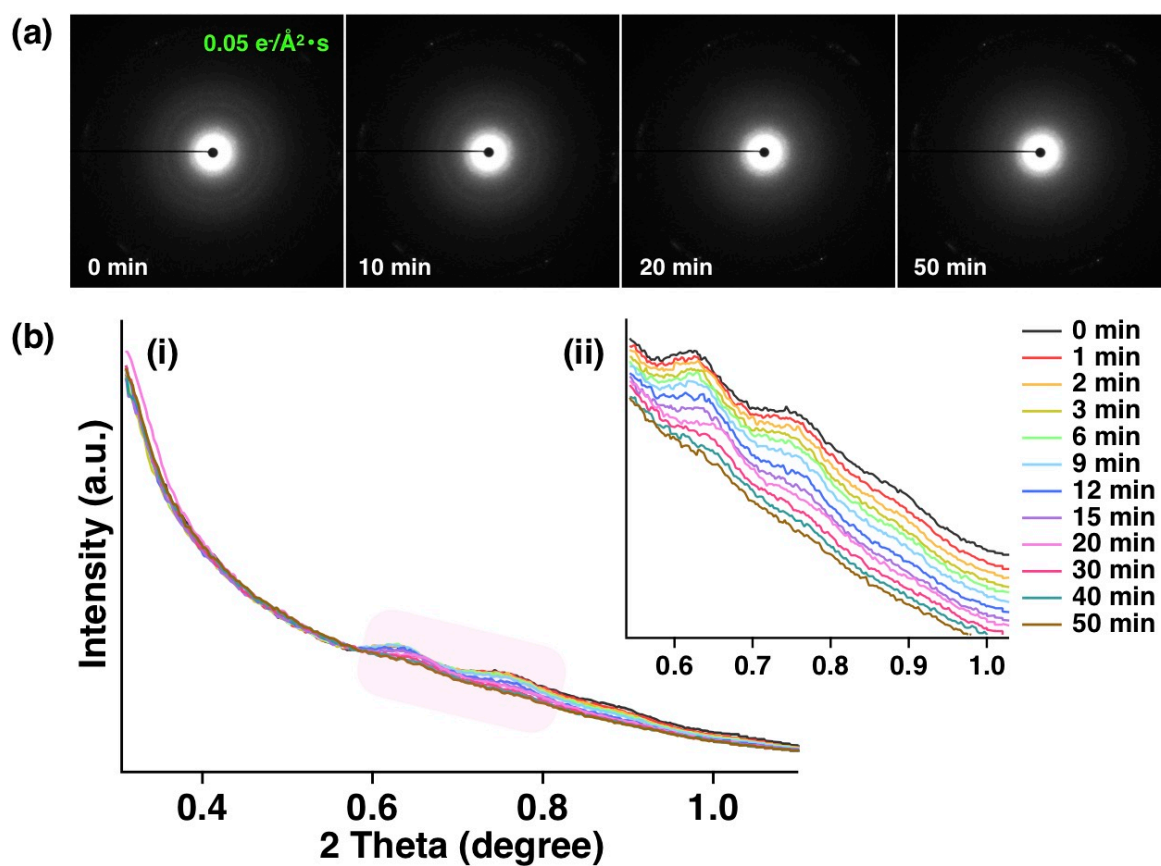


Figure S7. (a) Electron diffraction image of ZIF-7 aggregate with different irradiation time (electro dose rate: $0.05 \text{ e}^-/\text{\AA}^2 \cdot \text{s}$), (b-i) Electron diffraction patterns obtained by converting the Debye-rings and (ii) an extended figure (pink area).

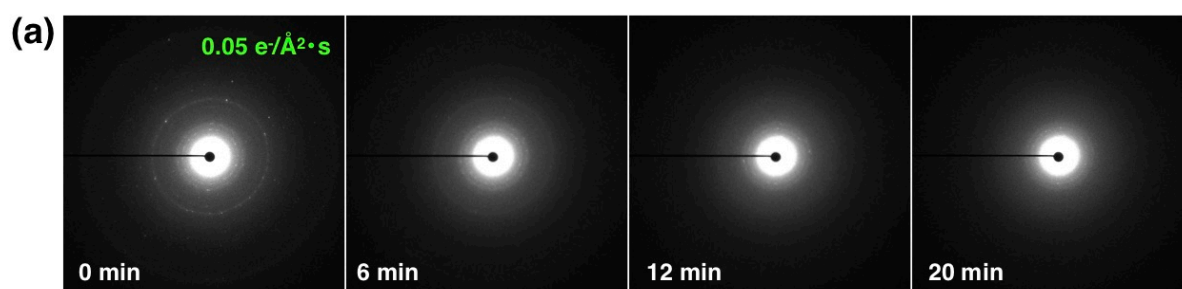


Figure S8. Electron diffraction image of UiO-67 aggregate with different irradiation time (electro dose rate: $0.05 \text{ e}^-/\text{\AA}^2 \cdot \text{s}$).

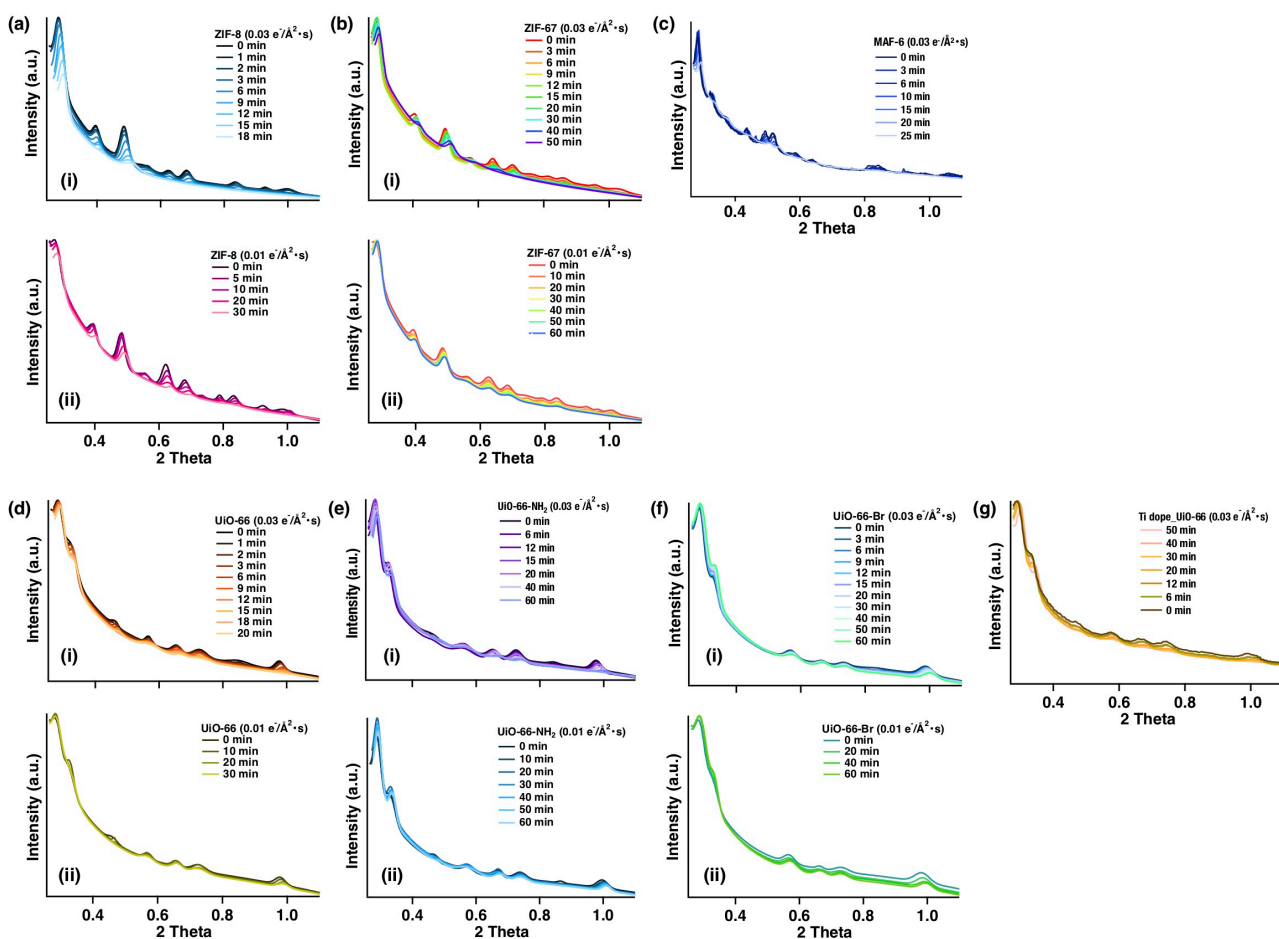


Figure S9. Electron diffraction patterns obtained by converting the Debye-rings of each samples: (a) ZIF-8, (b) ZIF-67, (c) MAF-6, (d) UiO-66, (e) UiO-66_{NH₂}, (f) UiO-66-Br₂ and (g) Ti-doped UiO-66 (electron dose rate: i_0.03 e⁻/Å²·s and ii_0.01 e⁻/Å²·s).

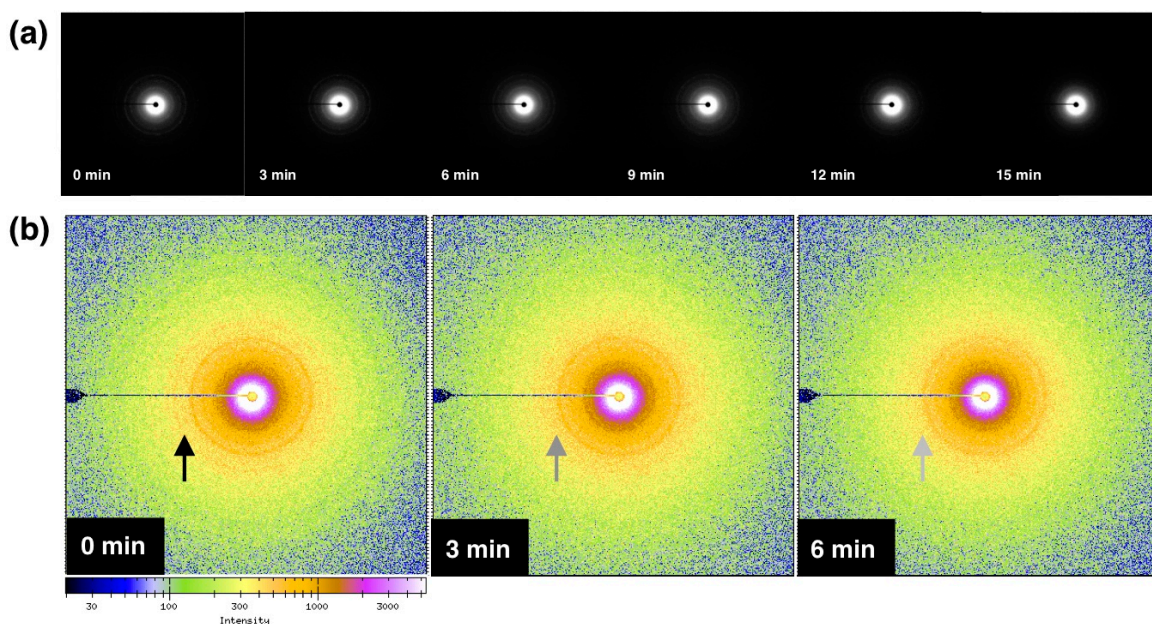


Figure S10. (a) Electron diffraction image of 50 nm-sized ZIF-8 with acceleration voltage of 80 kV (electron dose rate: 0.05 e⁻/Å²·s) and (b) electron diffraction images displayed in log-scale gradient color.

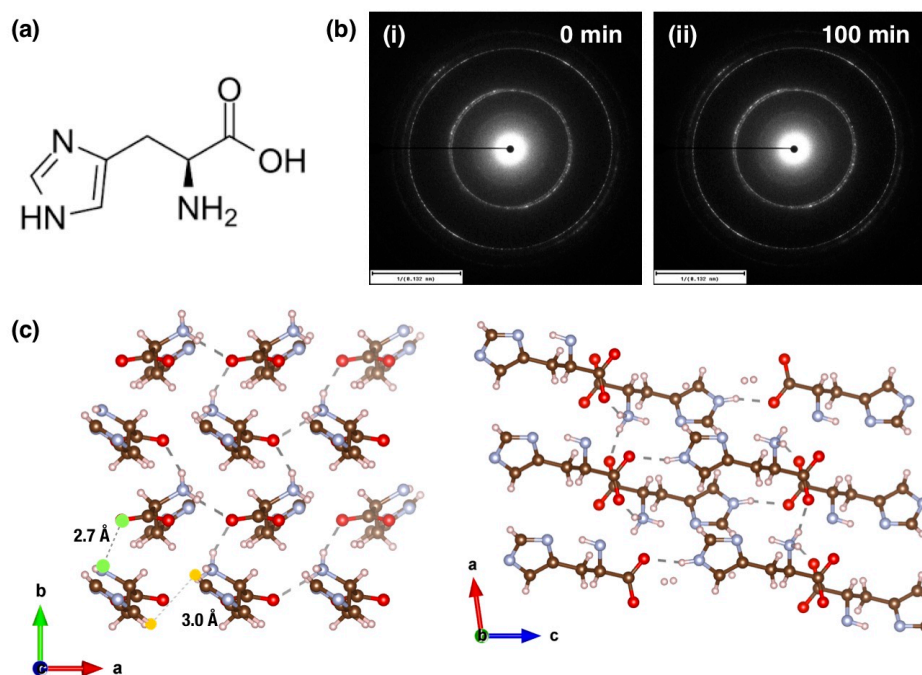


Figure S11. (a) Molecular structure, (b) Diffraction images with different irradiation time of *L*-histidine: (i)_0 min and (ii)_100 min (electron dose rate: $0.05 \text{ e}/\text{\AA}^2 \cdot \text{s}$) and (c) crystal structure of *L*-histidine (left: *c*-axis, right: *b*-axis).

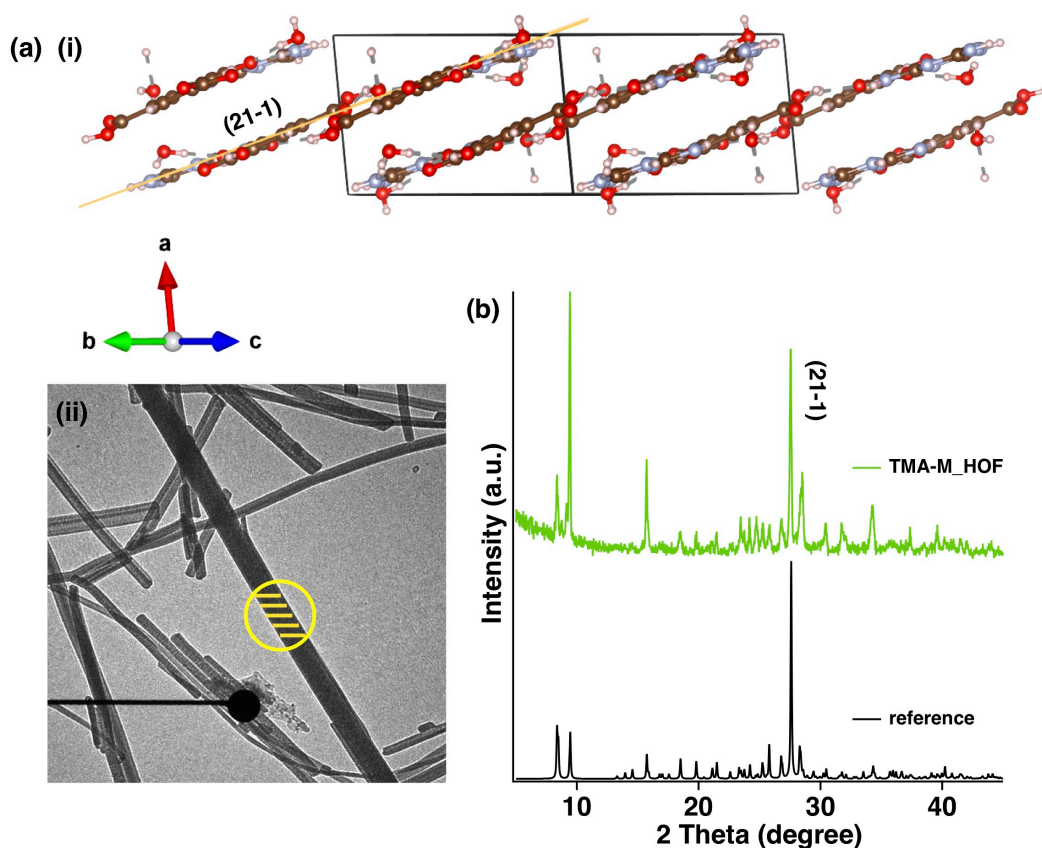


Figure S12. (a-i) A crystal structure of TMA-M HOF, (a-ii) a shadow image (shaded line: plane of [21-1], circle: rough observation area), and (b) PXRD patterns.

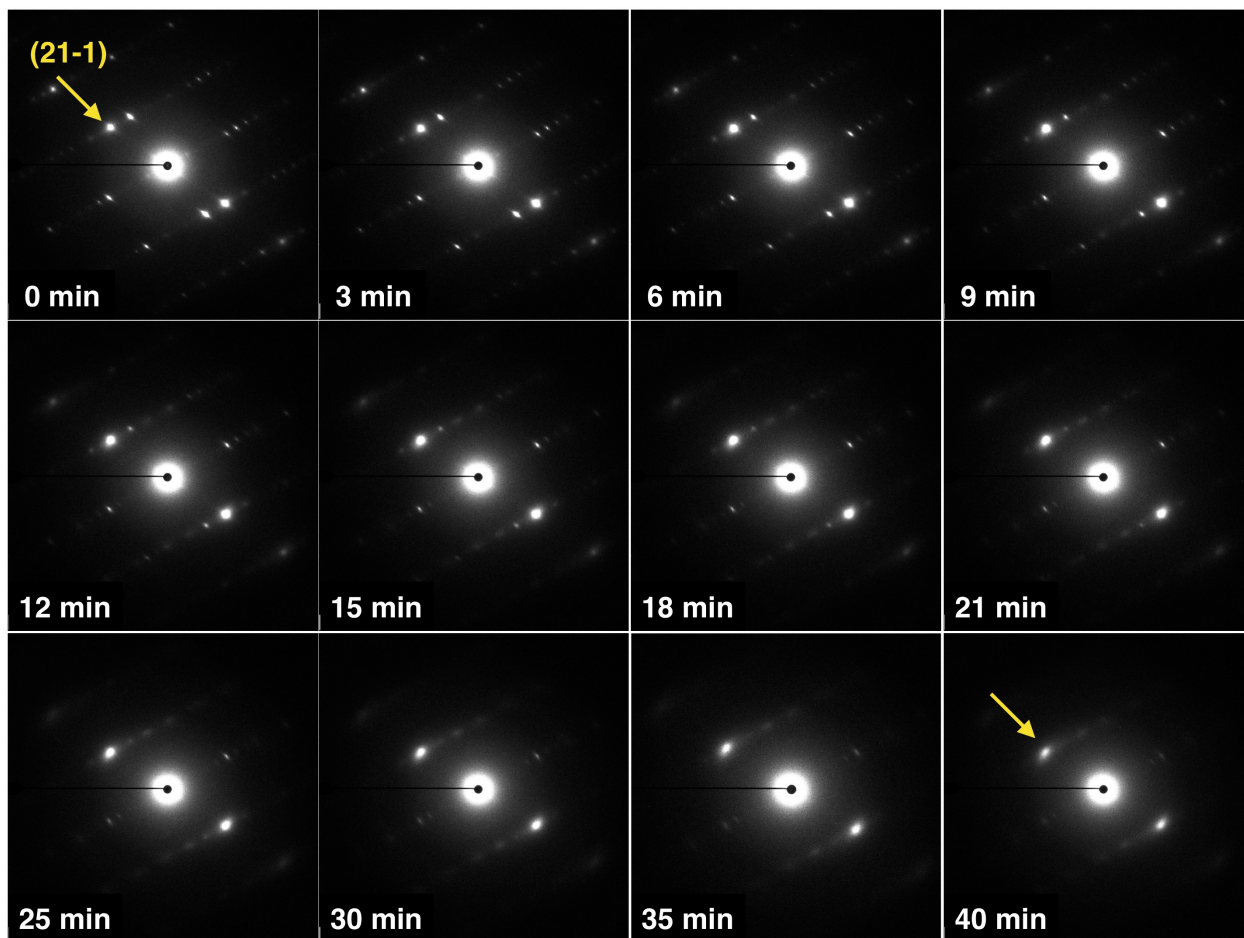


Figure S13. Electron diffraction image of TMA-M HOF (electron dose rate: $0.05 \text{ e}/\text{\AA}^2 \cdot \text{s}$).

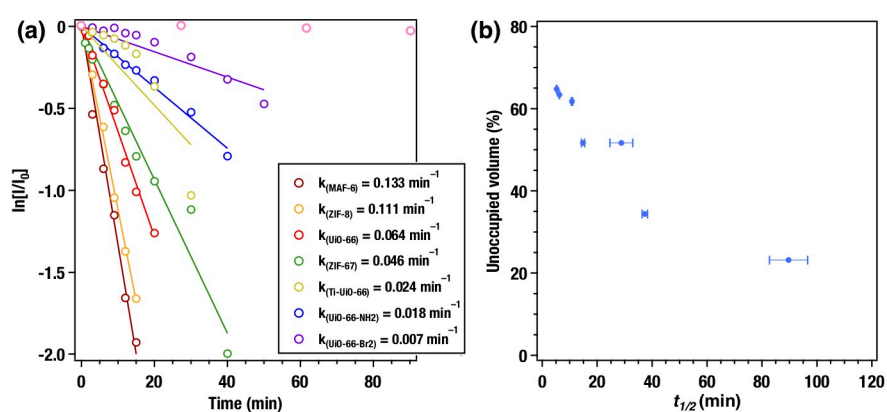


Figure S14. (a) First-order kinetic plots of time course change of normalized total electron diffraction peak areas (I : normalized total diffraction intensity, electron dose rate $0.05 \text{ e}/\text{\AA}^2 \cdot \text{s}$) and (b) correlation graph between unoccupied volume and half-life of each crystal.